



**QUEEN'S
UNIVERSITY
BELFAST**

Identifying consumer-resource population dynamics using paleoecological data

Einarsson, Á., Hauptfleisch, U., Leavitt, P. R., & Ives, A. R. (2016). Identifying consumer-resource population dynamics using paleoecological data. *Ecology*, 97(2), 361-371. <https://doi.org/10.1890/15-0596.1>

Published in:
Ecology

Document Version:
Peer reviewed version

Queen's University Belfast - Research Portal:
[Link to publication record in Queen's University Belfast Research Portal](#)

Publisher rights

Copyright 2016 Ecological Society of America. This work is made available online in accordance with the publisher's policies. Please refer to any applicable terms of use of the publisher.

General rights

Copyright for the publications made accessible via the Queen's University Belfast Research Portal is retained by the author(s) and / or other copyright owners and it is a condition of accessing these publications that users recognise and abide by the legal requirements associated with these rights.

Take down policy

The Research Portal is Queen's institutional repository that provides access to Queen's research output. Every effort has been made to ensure that content in the Research Portal does not infringe any person's rights, or applicable UK laws. If you discover content in the Research Portal that you believe breaches copyright or violates any law, please contact openaccess@qub.ac.uk.

1 **Identifying consumer-resource population dynamics using paleoecological data**

2

3

4 Árni Einarsson^{1,2}, Ulf Hauptfleisch^{1,3}, Peter R. Leavitt⁴, Anthony R. Ives⁵

5

6 ¹ Mývatn Research Station, IS-660 Mývatn, Iceland

7

8 ² Institute of Life- and Environmental Sciences, Askja, Sturlugata 7, University of Iceland, IS-101

9 Reykjavík, Iceland

10

11 ³ Faculty of Earth Sciences, Askja, Sturlugata 7, University of Iceland, IS-101 Reykjavík, Iceland

12

13 ⁴ Department of Biology, University of Regina, Regina, SK, Canada S4S 0A2

14

15 ⁵ Department of Zoology, University of Wisconsin, Madison, WI 53706, USA

16

17

18

19 ABSTRACT

20 Ecologists have long been fascinated by cyclic population fluctuations, because they suggest
21 strong interactions between exploiter and victim species. Nonetheless, even for populations
22 showing high-amplitude fluctuations, it is often hard to identify which species are the key drivers
23 of the dynamics, because data are generally only available for a single species. Here, we use a
24 paleoecological approach to investigate fluctuations in the midge population in Lake Mývatn,
25 Iceland, which ranges over several orders of magnitude in irregular, multi-generation cycles.
26 Previous circumstantial evidence points to consumer-resource interactions between midges and
27 their primary food, diatoms, as the cause of these high-amplitude fluctuations. Using a pair of
28 sediment cores from the lake, we reconstructed 26 years of dynamics of midges using egg
29 remains, and algal groups using diagnostic pigments. We analyzed these data using statistical
30 methods that account for both the autocorrelated nature of paleoecological data and measurement
31 error caused by the mixing of sediment layers. The analyses revealed a signature of consumer-
32 resource interactions in the fluctuations of midges and diatoms: diatom abundance (as inferred
33 from biomarker pigment diatoxanthin) increased when midge abundance was low, and midge
34 abundance (inferred from egg capsules) decreased when diatom abundance was low. Similar
35 patterns were not found for pigments characterizing the other dominant algal group in the lake
36 (cyanobacteria), subdominant algae (cryptophytes), or ubiquitous but chemically unstable
37 biomarkers of total algal abundance (chlorophyll-*a*); however, a significant but weaker pattern
38 was found for the chemically stable indicator of total algal populations (β -carotene) to which
39 diatoms are the dominant contributor. These analyses provide the first paleoecological evaluation
40 of specific trophic interactions underlying high amplitude population fluctuations in lakes.

41

42 Key words: fossil pigments; Lake Mývatn; Chironomidae; diatoms; population fluctuations;
43 consumer-resource dynamics; Iceland.

44

INTRODUCTION

45
46 Cyclic population dynamics have generated one of the oldest and largest bodies of
47 literature in ecology, starting with the classic models of Lotka showing that population cycles can
48 be generated by predator-prey, or more generally, exploiter-victim interactions (Lotka 1925).
49 Population cycles have generated this interest because they are an easily observed signal of
50 strong interactions among species (Kendall et al. 1999). Despite the numerous population cycles
51 that have been documented, in many cases it is unclear what are the key species driving the
52 cycles. For the iconic snowshoe hare cycles, only extensive research over many decades led to
53 the generally accepted hypothesis that cycles are driven primarily by predation from lynx and
54 other specialist predators, with secondary importance attributed to interactions with the hare food
55 base (Krebs et al. 1995, Krebs 2011). At high latitudes, cycles of microtine rodent populations
56 are common, yet there is still debate over the relative importance of top-down interactions
57 between rodents and predators in driving the cycles (Stenseth 1999, Turchin and Hanski 2001).
58 For insects, numerous cyclic populations have been documented, especially among forest pests;
59 the majority are explained by interactions with predators or parasites, although the identities of
60 the predators or parasites are often just speculations (Myers 1988, Turchin 2003, Turchin et al.
61 2003, Dwyer et al. 2004). Identifying the interactors who generate cycles between herbivores and
62 plants might be easier given the sedentary nature of plants, but with a few exceptions (Berryman
63 1976, Berryman et al. 1978), herbivore-plant cycles appear rare. Finally, although there is
64 considerable data on both zooplankton and phytoplankton in lakes, cyclic dynamics that are
65 sustained across multiple years (rather than the well-known annual clear-water period caused by
66 high consumption rates following spring turnover) are apparently rare (Murdoch et al. 1998),
67 despite the ability to find these cycles in the lab (McCauley et al. 1999, McCauley et al. 2008).

68 Thus, understanding most of the population cycles observed in nature is hampered by the absence
69 of data on a candidate partner species.

70 Almost 40 years of ecological monitoring in Lake Mývatn, Iceland, have revealed high-
71 amplitude fluctuations in the abundance of midges (chironomids) that span several orders of
72 magnitude (Einarsson et al. 2002, Einarsson and Gulati 2004, Gardarsson et al. 2004). Because
73 midges make up more than 90% of the secondary production of the lake benthos (1972-1974,
74 Lindegaard and Jónasson 1979), the fluctuations generate huge changes to the trophic structure of
75 the lake and drive fluctuations throughout the lake food web (Einarsson and Gulati 2004). The
76 midge fluctuations are cyclic, in the sense that they show clear, multi-generational peaks and
77 troughs, yet they are not strictly periodic, because the time between consecutive peaks ranges
78 from 4 to 7 years (Gardarsson et al. 2004).

79 Indirect evidence suggests that fluctuations of the dominant midge species, *Tanytarsus*
80 *gracilentus* Holmgren, are driven by resource interactions with their primary food, benthic
81 diatoms and detritus (Ingvason et al. 2004). While almost all of the 20 species of midges in the
82 lake show synchronous population fluctuations, the fluctuations of *T. gracilentus* are the most
83 extreme (5 orders of magnitude) and, at peak abundances, this species makes up roughly 80% of
84 the midge population by numbers (Gardarsson et al. 2004). In the 23-year (46-generation) time
85 series from 1977 to 1999, the adult body size of *T. gracilentus* decreased during the generations
86 before population collapse, suggesting resource limitation leading up to troughs in the cycles
87 (Einarsson et al. 2002). Furthermore, a mathematical model of *T. gracilentus*-diatom-detritus
88 interactions that was fit to time-series data on adult midge fluctuations revealed complex
89 dynamics with alternative states representing either a high-amplitude cycle or a moderately high
90 stable point; the irregular period of midge fluctuations could be explained by the midge
91 population exiting the high-amplitude cycles to spend a stochastic duration of time near the stable

92 point (Ives et al. 2008). While these empirical and theoretical results support the hypothesis that
93 midge fluctuations arise from consumer-resource interactions within Lake Mývatn, they are
94 based solely on data from fluctuations in adult midges. No information has been available to test
95 whether diatom dynamics are consistent with exploiter-victim cycles.

96 Here, we use the hindsight offered by paleoecological methods to test whether the
97 dynamics of midges and benthic diatoms could be the result of consumer-resource interactions.
98 Paleoecological approaches are typically used to address ecosystem-level questions, because they
99 provide synoptic information about a system (Smol 2010). This retrospective approach has been
100 used successfully to quantify both algal periodicity (Carpenter and Leavitt 1990) and
101 invertebrate-algal interactions (Leavitt et al. 1989), but never to evaluate the interaction between
102 the two. Here, we combine approaches for the first time, develop novel state-space models to
103 measure reciprocal interactions between herbivores and their resources, and test the population-
104 level hypothesis that fluctuations in diatom and midge abundances are consistent with dynamics
105 expected in tightly coupled consumer-resource interactions. We analyzed two sediment cores
106 from Lake Mývatn representing the period 1975-2003. This time period corresponds closely to
107 our data on midge abundances obtained through trapping adults that began in 1977, and
108 Hauptfleisch et al. (2012) validated the estimates of midge abundances obtained from
109 sedimentary egg counts against the monitoring estimates of adult abundances. From a second
110 core we assayed an array of pigments representing diatoms (diatoxanthin), cyanobacteria that
111 occur in the water column and therefore are not a major component of midge food (echinenone),
112 subdominant cryptophytes (alloxanthin) not heavily consumed by midges, and general indicators
113 of algal abundance that exhibit either robust chemical stability (β -carotene) or are highly labile

114 (chlorophyll-*a*) (Leavitt and Hodgson 2001). We anticipated that only diatoms would show
115 dynamics consistent with consumer-resource cycles.

116 To assess the dynamics of midges (egg capsules) and primary producers (pigments), we
117 first analyzed the temporal correlations between these variables. These correlation analyses are
118 complicated by autocorrelation, the tendency of many time series to show correlations between
119 successive samples. Although the complications introduced by autocorrelation are well-known in
120 the statistical and ecological literature, only recently have these complications been
121 acknowledged in the paleoecological literature (Blaauw et al. 2010). We then address the more
122 specific question of whether diatoms increase in abundance when midges are rare and whether
123 midges decrease in abundance when diatoms are rare. The midge population peaks that occur
124 every 4-7 years accentuate the problem of sediment mixing that confronts all paleoecological
125 studies; biotic and abiotic disturbances mix the sediment so that a given stratum contains a
126 mixture of material deposited at different times. This is a form of measurement error that can blur
127 a signal, especially by spreading peaks or filling troughs in the cyclic fluctuations of the variables
128 of interest (Leavitt and Carpenter 1989). Therefore, we developed a statistical method that
129 accounts for sediment mixing to give a more-accurate depiction of population time series from
130 sediment cores. Our overall goal is to show how paleoecological approaches can resurrect
131 historical patterns of population dynamics, provided requisite statistical care is given. In our
132 specific case, we use this approach to give the first direct evidence that consumer-resource
133 interactions could drive the sustained, multi-year fluctuations in midge population dynamics
134 found in Lake Mývatn.

135

136

METHODS

137

Study system

138 Lake Mývatn is situated in northeastern Iceland at 65°6`N and 17°00`W in an active
139 volcanic area formed by basaltic lava flows (Thorarinsson 1979). Most of the inflow is from
140 groundwater flowing through lava fields, and the resulting high nutrient inputs make the lake
141 highly eutrophic. The maximum natural depth is 4.2 m, with an average depth of 2.5 m. The lake
142 is divided into a north basin (8.5 km²) and a south basin (28.2 km²). Water inflow is
143 predominantly from cold and warm springs along the eastern shore. Due to its passage through
144 volcanic basalts, the spring waters contain high concentrations of phosphate (1.62 μM), silica and
145 other dissolved solids, and have a pH ranging between 8.3 and 9.2 (Ólafsson 1979a). The water
146 column is well mixed during the summer months, while thermal stratification and hypoxia occur
147 locally in mid winter (Ólafsson 1979b).

148 The Icelandic name Mývatn means midge lake after its enormous chironomid swarms.
149 During high-midge years, *T. gracilentus* is by far the most abundant midge species. It has two
150 generations per year, with adults emerging over a 2-3 week period in each of June and late July-
151 August. Gut content analysis of *T. gracilentus* shows a diet of roughly equal parts diatoms and
152 detritus (Ingvason et al. 2004), with much of the detritus likely frass from previous generations
153 and hence coming ultimately from diatoms. Total net primary production for Lake Mývatn in
154 1972-1973 was about 350 g C/m²/yr (Jonasson 1979, Jonasson and Adalsteinsson 1979), with
155 most of this from benthic diatoms (220 g C/m²/yr based on the 1973-1974 silica budget of the
156 lake, Ólafsson 1979a); in 2000-2001, Thorbergsdóttir et al. (2004) estimated total benthic
157 production of 250 and 340 g C/m²/yr at two sites using in situ oxygen flux chambers. In addition,
158 extensive lake floor areas of the south basin exhibit loose mats of filamentous green algae
159 (Cladophorales), the extent of which varies greatly on a decadal scale (Einarsson et al. 2004).
160 Blooms of cyanobacteria (*Anabaena spp.*) occur in most years (Jonasson and Adalsteinsson 1979,
161 Einarsson et al. 2004).

162

163

Coring and sampling

164

165

166

167

168

169

170

171

172

173

174

175

Two 5-cm diameter sediment cores were retrieved using a Kajak-Brinkhurst corer (Brinkhurst et al. 1969) from 3.75-m deep sites <1 m apart in a sheltered bay, *Breida by Höfði*, on the east side of Lake Mývatn in June 2006 (Fig. 1). Cores KB-1 and KB-2 were 32- and 34-cm long, respectively, and composed of diatomaceous gyttja (Troels-Smith 1955, Aaby and Berglund 1986), or massive and very moist diatomaceous ooze in the terminology of Schnurrenberger et al. (2003). Core KB-1 was analyzed for loss on ignition (LOI) and arthropod microfossils (cladoceran exuviae and chironomid egg capsules) by Hauptfleisch et al. (2012). Core KB-2 was used for the pigment analysis presented here. The cores were extruded in a vertical position aboard the boat, the outermost 0.5-cm layer of smearing was removed with a spatula, and they were then sliced at 0.5-cm intervals. The samples were placed in plastic bags, sealed and transported in a cooler box immediately to the laboratory on the lakeshore where they were stored at 4°C.

176

177

178

179

180

181

182

183

184

For cores KB-1 and KB-2, we first removed the uppermost 10 cm, as these sediments were highly flocculent and largely uncompacted. The time scale of the cores was fine-tuned by matching the profile of the sediment with known events including documented peaks in chironomid abundances (1979, 1987, 1992, 2000) and a tephra layer from an eruption in Grimsvotn volcano in 2004 (Hauptfleisch et al. 2012). We regressed the time of these events against core depth using a quadratic curve, and all results are subsequently presented in terms of this time scale. The analyzed sections of the cores represent the time period 1975-2004, and the time intervals corresponding to 0.5-cm slices ranged from 0.81 yr at the bottom of the core to 0.30 yr at the top, reflecting compaction of the lower sediments.

185 To estimate water content and organic matter content, 1 ml of wet sediment was placed in
186 ceramic crucibles and dried at 80°C for 24 h. The dried samples were combusted in a preheated
187 furnace at 550°C for 1 h, cooled in a desiccator for 30 min, and weighed at room temperature
188 (Håkanson and Jansson 1983). For additional background data, diatom proportions (*Fragilaria*
189 spp. vs. non-*Fragilaria* spp.) were counted in the combusted sediment samples.

190

191 *Pigments*

192 Algal abundance was quantified from fossil pigments and their derivatives. Pigments
193 were extracted from lyophilized (48 h, 0.01 Pa) whole sediment samples, filtered (0.2- μ m pore),
194 and dried under pure N₂ gas using the standard methods of Leavitt and Hodgson (2001).
195 Diatoxanthin, echinenone, alloxanthin, β -carotene, and chlorophyll-*a* were isolated and
196 quantified using an Agilent model 1100 high-performance liquid chromatography (HPLC)
197 system equipped with photo-diode array and fluorescence detectors, and calibrated with authentic
198 standards. All pigment concentrations are expressed as nmol pigment/g sediment C, a metric
199 which is linearly correlated to annual algal standing stock in whole-lake calibration studies
200 (reviewed in Leavitt and Hodgson 2001).

201

202 *Chironomid eggs*

203 We used chironomid eggs as a proxy for chironomids, because they are much more
204 abundant in the sediment and easier to handle than larval head capsules. Egg capsules cannot be
205 identified to species, however, so we cannot separate the different species of midges. For
206 counting, 2 ml of wet sediment were deflocculated by heating in 10% KOH (weight/volume) at
207 80°C for 2 h and sieved through a 63- μ m mesh. The residue was separated by floatation in water

208 into animal exoskeletal fragments and sand grains. Chironomid egg capsules were identified by
209 their oval, usually slightly asymmetrical shape and smooth surface. The results of the analysis of
210 chironomid egg capsules were published by Hauptfleisch et al. (2012).

211

212 *Correlations among variables*

213 We first analyzed the correlations among variables through time. Standard statistical tests
214 of the significance of correlations between two variables Y_1 and Y_2 assume that the values of the
215 variable Y_1 are independent of each other, as are the values of Y_2 . However, biological processes
216 are often autocorrelated through time; midge and algal abundances might remain at high or low
217 levels for months or years (Einarsson et al. 2004, Gardarsson et al. 2004). Because positive
218 autocorrelation causes a variable of interest to fluctuate slowly over the possible range of values
219 it can take, autocorrelation can increase type I errors (false positives) in statistical tests of
220 correlation between two variables.

221 To account for possible temporal autocorrelation, we performed the following parametric
222 bootstrap procedure. We first fit an autoregressive-moving average (ARMA) model to each time
223 series. ARMA(p,q) models have the form

$$224 \quad y(t) - \mu = \sum_{i=1}^p \beta_i (y(t-1) - \mu) + \sum_{j=0}^q \alpha_j \varepsilon(t-j) \quad (1)$$

225 where $y(t)$ is the value of a variable in sediment stratum t , μ gives the mean of $y(t)$, β_i are the
226 autoregressive coefficients, ε_t is a temporally independent random variable, and α_j are the moving
227 average coefficients (Box et al. 1994, Ives et al. 2010). Thus, the first term on the right-hand side
228 is the autoregressive component of the model, and the second term is the moving average
229 component; the greater the values of p and q , the longer the time lags included in the AR and MA

230 components of the model. ARMA models are flexible enough to fit potentially complex patterns
231 of autocorrelation (Ives et al. 2010), and we used Akaike's Information Criterion corrected for
232 small sample sizes (AICc) to select the values of p and q that give the best fits to the time series.
233 We then simulated data from the best-fitting ARMA models and computed pairwise Pearson's
234 correlation coefficients from the simulated data sets. Repeating this for 100,000 simulated data
235 sets gives the approximate distribution of the estimator (Efron and Tibshirani 1993) of the
236 correlation coefficient under the null hypothesis that the time series $y_1(t)$ and $y_2(t)$ are
237 independent but temporally autocorrelated, and we used this to compute p-values. Because we
238 were interested in fluctuations in the response variables, we detrended the response variables with
239 a quadratic function, $y(t) = c_0 + c_1 t + c_2 t^2$, and standardized the residuals to have standard
240 deviation 1 (Patoine and Leavitt 2006). This removes possible degradation or transformation of
241 pigments through time.

242 When considering correlations among several variables, we also used the bootstrap
243 procedure to obtain p-values corrected for multiple comparisons using an approach comparable to
244 a sequential (Holm) Bonferroni correction (Holm 1979). We first ordered the K correlation
245 coefficients from lowest to highest p-value. For the first correlation coefficient, we counted the
246 proportion of simulated data sets (including all variables) for which one or more of the K
247 correlation coefficients had a lower p-value; this proportion gives the corrected p-value for the
248 first correlation coefficient. We then excluded this correlation coefficient from the simulated data
249 sets and repeated the procedure for the second correlation coefficient, asking what proportion of
250 the simulated data sets had one or more of the $K - 1$ p-values lower than the observed p-value of
251 the second correlation coefficient. We repeated this procedure, excluding correlation coefficients
252 until the corrected p-value exceeded 0.05. This approach allowed us to report p-values that
253 account for the multiple correlation coefficients we computed.

254

255

State-space model

256

257

258

259

260

261

262

263

264

265

266

267

268

269

270

271

272

273

274

275

Whereas our parametric bootstrap procedure gives a statistically valid method for assessing correlations among variables, we also wanted to test the more-mechanistic hypothesis that high midge abundance (egg capsules) caused diatom abundance (diatoxanthin) to decrease, while high diatom abundance allowed midges to increase. For this we designed a state-space model (Harvey 1989) that explicitly incorporates both autocorrelation and measurement error generated by sediment mixing. We performed analyses not only for diatoxanthin, but also for echinenone, alloxanthin, β -carotene, and chlorophyll-*a*; we expected the strongest interaction between midges and diatoms, so these other pigments serve as statistical controls. Note, however, that they are not independent; for example, diatoms contain not only diatoxanthin but also β -carotene and chlorophyll-*a*. Differences in chemical stability of the latter two pigments allowed us to evaluate whether our approach was additionally subject to diagenetic effects of post-depositional pigment degradation. As reviewed in Leavitt and Hodgson (2001), the carotenoids used in this study are all well preserved in lake sediments, in contrast to ubiquitous chlorophyll-*a* which is rapidly transformed or discolored in surface deposits.

The state-space model comprises two sets of equations, one describing process error (biological variability) and the other measurement error (including vertical mixing of sediment).

The process equations are

$$\begin{aligned} \log x_1(t) &= b_{10} + \tau(t) \left[b_{11} (\log x_1(t-1) - b_{10}) + b_{12} \log x_2(t-1) \right] + \varepsilon_1(t) \\ \log x_2(t) &= b_{20} + \tau(t) \left[b_{22} (\log x_2(t-1) - b_{20}) + b_{21} \log x_1(t-1) \right] + \varepsilon_2(t) \end{aligned} \quad (2)$$

where $\log x_1(t)$ is the natural logarithm of the concentration of the algal pigment of interest, and $\log x_2(t)$ is log midge egg capsule abundance. We modeled variables on a log scale because we

276 expect ecological processes to act multiplicatively; taking the log allows the use of a linear
 277 autoregressive model and is formally equivalent to a Gompertz multiplicative population model
 278 (Dennis and Taper 1994). The samples t give the consecutive 0.5-cm core slices rescaled to time
 279 in years (see *Methods: Coring and sampling*). To account for sediment compaction, $\tau(t)$ gives the
 280 time interval between the core samples at $t-1$ and t . The Gaussian random variables $\varepsilon_i(t)$ with
 281 means zero and variances σ_i^2 represent variation in $\log x_i(t)$ between samples. The coefficients b_{i0}
 282 give the expected value of $\log x_i(t)$, b_{ii} measures the autocorrelation of $\log x_i(t)$ from one sample
 283 to the next, and b_{ij} measures the effect of $\log x_j(t)$ on $\log x_i(t)$; thus, if b_{12} is negative, then high
 284 midge abundances are associated with decreases in log pigment concentration between samples t
 285 and $t + 1$, and if b_{21} is positive, then high pigment concentrations are associated with increases in
 286 log midge egg capsules.

287 The measurement equations are

$$\begin{aligned}
 x_1(t)^* &= \sum_{T=0}^r a^T x(t-T) + \phi_1(t) \\
 x_2(t)^* &= \sum_{T=0}^r a^T u(t-T) + \phi_2(t)
 \end{aligned}
 \tag{3}$$

289 where $x_1(t)^*$ and $x_2(t)^*$ are the observed values of $x_1(t)$ and $x_2(t)$ at time t . Because mixing of
 290 sediment is an additive process, the measurement equations are formulated using the
 291 untransformed values of $x_1(t)$ and $x_2(t)$. To account for sediment mixing, the observed values
 292 $x_1(t)^*$ and $x_2(t)^*$ depend not only on the sedimentation rates of $x_1(t)$ and $x_2(t)$ at sample t , but also
 293 on the sedimentation for r core increments into the past (lower sediments). The sedimentation
 294 rates T time steps in the past are discounted by the term a^T ($a < 1$), so that spatially more-distant
 295 sediments have lower mixing with the sediments in sample t . This equation makes the
 296 simplifying approximation that the sediments in sample t are mixed with lower sediments but not

297 with sediments above; while this is the case immediately following the deposition of sediment,
298 later mixing with higher sediments will occur (Leavitt and Carpenter 1989). We address this
299 asymmetry in more detail with simulations in Appendix A (online Supplemental Material).
300 Finally, $\phi_1(t)$ and $\phi_2(t)$ are Gaussian random variables with variances $x_1(t)v_1^2$ and $x_2(t)v_2^2$. These
301 variances are proportional to the mean under the assumption that sampling variability is
302 approximately Poisson; this also prohibits negative values of $x_1(t)^*$ and $x_2(t)^*$ when the predicted
303 values of $x_1(t)$ and $x_2(t)$ are small. Because separate cores were taken for algal pigments and
304 midge egg capsules, we assumed zero correlation between $\phi_1(t)$ and $\phi_2(t)$.

305 We fit the state-space model given by equations 2 and 3 using an extended Kalman filter
306 to calculate the likelihood function (Harvey 1989). Maximum likelihood parameter values were
307 estimated for 11 variables: b_{10} , b_{20} , b_{12} , b_{21} , b_{11} , b_{22} , a , σ_1^2 , σ_2^2 , v_1^2 , and v_2^2 . We tested the
308 statistical significance of the effect of midge abundance on pigments, b_{12} , and pigments on midge
309 abundance, b_{21} , using likelihood ratio tests to compare the full 11-parameter model with the
310 reduced 9-parameter model in which $b_{12} = b_{21} = 0$, as well as the separate 10-parameter models
311 with either $b_{12} = 0$ or $b_{21} = 0$. Likelihood ratio tests are based on the asymptotic approximation
312 that with large sample sizes, the log-likelihood ratios are χ^2 distributed with degrees of freedom
313 equal to the difference in the number of parameters between models (Harvey 1989). We
314 performed these analyses for $r = 3$ which sets the maximum mixing distance at 3 core sections (2
315 cm). To account for possible trends in variables through time, we first quadratically detrended all
316 variables. After detrending, we added a constant to each time series to give it the same minimum
317 value as the non-detrended time series, and then standardized to give each time series a variance
318 of one. For fitting the model, we assumed that the initial values of $x_i(0)$ were their observed
319 values. The initial variances of $\log x_1(0)$ and $\log x_2(0)$ were set to σ_1^2 and σ_2^2 , with zero

320 covariance. Our statistical approach allows direct evaluation of whether the dynamics of midges
321 and algae observed in the sediment are consistent with strong consumer-resource interactions.

322

323 *Validation using a simulation model*

324 Because the midge dynamics inferred from adult data are not strictly periodic, we tested
325 whether the state-space approach (Eqs. 2, 3) could detect negative effects of midges on diatoms
326 and positive effects of diatoms on midges even for non-periodic data that we would expect in
327 Lake Mývatn. We generated simulated core data by predicting midge and diatom abundances
328 from the midge-diatom-detritus model that we previously fit to the adult midge time series (Ives
329 et al. 2008); this model showed possible alternative states underlying *Tanytarsus gracilentus*
330 dynamics. Using the model to generate midge and diatom abundances, we then simulated the
331 sedimentation process including both deposition and mixing between adjacent sediment layers;
332 details are given in Appendix A (online Supplemental Material). We fit the simulated data using
333 the same procedure as we used for the real sediment core data. If the model fit to simulated data
334 gives similar results to those when fit to the real data, then we can be confident that our approach
335 will detect consumer-resource interactions even when these interactions do not lead to cycles
336 with regular periods.

337

338 RESULTS

339 Our analyses focus on the interactions between midge abundance (egg capsules) and the
340 abundances of diatoms (diatoxanthin), cyanobacteria (echinenone), cryptophytes (alloxanthin),
341 and total algal abundance as recorded by chemically stable (β -carotene) and labile biomarkers
342 (chlorophyll-*a*) (Appendix B, Fig. B1). As expected, the strongest correlations were recorded

343 between the two markers of total algal abundance, as well as total algal abundance and the
344 predominant benthic (diatom) and planktonic (cyanobacteria) algal groups (Table 1). Weaker
345 correlations were observed between planktonic cyanobacteria (echinenone) and cryptophytes
346 (alloxanthin). In contrast, only concentrations of the pigment diatoxanthin (diatoms) were
347 correlated significantly (-0.37) with midge egg capsules (Table 1).

348 Statistical significance of these correlations (Table 1) was determined by parametric
349 bootstrapping to account for autocorrelation in the individual time series. We also computed p-
350 values using standard Pearson correlation coefficients (Table 2). In all cases the p-values ignoring
351 autocorrelation were smaller than those computed when accounting for autocorrelation; for
352 example, the standard p-value for the correlation of -0.37 between midge egg capsules and
353 diatoxanthin was 0.012, whereas the bootstrap estimate was 0.039. This comparison underscores
354 the need to account for autocorrelation when comparing fossil time series.

355 Diatoxanthin showed peaks in 1977, 1983, 1987, and 1999 that preceded peaks in midge
356 egg capsule counts (Fig. 2). This pattern is consistent with consumer-resource interactions in
357 which increases in diatoms occur at low midge abundance, and increases in midges occur at high
358 diatom abundance. In the state-space model (Eqs. 2, 3) the estimate for the effect of midges on
359 diatoxanthin is $b_{12} = -0.90$, and the effect of diatoxanthin on midges is $b_{21} = 0.46$ (Table 3); both
360 of these coefficients are significantly different from zero separately (b_{12} : $\chi^2_1 = 13.08$, $P = 0.0003$;
361 b_{21} : $\chi^2_1 = 6.46$, $P = 0.011$) and together ($\chi^2_2 = 26.84$, $P < 0.0001$). In addition, the analysis of
362 midge egg capsules and β -carotene gave a negative estimate of $b_{12} = -0.54$ ($\chi^2_1 = 9.79$, $P =$
363 0.0017) and a positive estimate of $b_{21} = 0.33$ ($\chi^2_1 = 4.04$, $P = 0.044$), similar to but weaker than
364 the interactions inferred between midges and diatoxanthin. None of the other pigments showed
365 statistically significant values of b_{12} and b_{21} , suggesting that the associated algae were not

366 involved in consumer-resource cycles (Table 3). Furthermore, the absence of significant
367 estimates if b_{12} and b_{21} for ubiquitous chlorophyll a confirms that models can be influenced by
368 post-depositional degradation of fossil records.

369 The state-space model fit to midge egg capsules and diatoxanthin gives information not
370 only about interaction strengths b_{12} and b_{21} , but also about other properties inferred from the data.
371 The best-fitting state-space model (Table 3) gave an estimate of $a = 0.55$ ($\chi^2_1 = 9.13$, $P = 0.0025$).
372 This value of a implies that 0.50 of the diatoxanthin remained in the sediment stratum where it
373 was deposited, while 0.27 ($= a/(1+a+a^2+a^3)$), 0.15, ($= a^2/(1+a+a^2+a^3)$) and 0.08 ($= a^3/(1+a+a^2+a^3)$)
374 represent sediment from slices 0.5, 1.0, and 1.5 cm below the observed core slice. This value of a
375 is similar for other pigments, except for the lower value estimated for echinenone. The fitted
376 value of b_{11} is close to zero, implying that there is little autocorrelation in diatom abundances
377 through time that is not explained by midge abundance; in contrast, $b_{22} = 1.29$, implying strong
378 autocorrelation in midge abundance. In contrast to these model parameters, other model
379 parameters were not informative. Specifically, the magnitudes of the process and sampling errors
380 (σ^2_i and v^2_i) often traded off against each other, so that $\sigma^2_i > 0$ and $v^2_i = 0$, or $\sigma^2_i = 0$ and $v^2_i > 0$.
381 This is the result of the difficulty of statistically separating process error from measurement error.

382 To validate the state-space modeling approach, we simulated midge and diatom
383 abundance data using the model that had been fit to adult *T. gracilentus* data collected during
384 1977-2002 (Ives et al. 2008), and then simulated the sedimentation process including mixing
385 among layers (Appendix A). As we found for the real core data, the analysis of the simulated core
386 data identified a negative value of $b_{12} = -0.55$ and positive value of $b_{21} = 0.82$, both of which
387 were statistically significant. The simulations show that the state-space model (Eq. 2 and 3) is

388 robust to pronounced but complex (aperiodic) variation in population abundance caused by
389 consumer-resource interactions.

390

391 DISCUSSION

392 Paleocological analysis of fossil midges (egg capsules) and diatoms (diatoxanthin)
393 provided direct support for the hypothesis that the dramatic midge population fluctuations in
394 Lake Mývatn are driven mainly by consumer-resource interactions between midges and their
395 food. Our state-space model showed that high midge egg capsule densities were associated with
396 decreases in diatoxanthin concentration and, in turn, high diatoxanthin concentrations were
397 associated with increases in midges. Furthermore, β -carotene (algae) showed a similar though
398 weaker pattern, consistent with the fact that diatoms are a main component of the algal
399 assemblage, and that changes in concentration of diatoxanthin and β -carotene were highly
400 correlated (Table 1). In contrast, none of other pigments showed significant correlation with
401 midge abundance.

402 Although concomitant changes in diatoms and midges do not prove that consumer-
403 resource interactions underlie the observed decadal-scale population fluctuations, several lines of
404 evidence suggest that population fluctuations are not driven by other trophic interactions within
405 Lake Mývatn. Two other general possibilities are bottom-up effects on diatoms (i.e., some other
406 interaction drives diatom fluctuations, and midges follow) and top-down effects on midges (i.e.,
407 some other interaction drives midge fluctuations, and diatoms follow). For the bottom-up
408 alternative, there would have to be a driver of diatom fluctuations other than midges. Diatoms are
409 the dominant group of primary producers in the lake, accounting for over 50% of primary
410 production (see *Methods: Study system*). Furthermore, most primary production is benthic rather

411 than pelagic, and diatoms are the dominant benthic primary producers (>95% of them are benthic
412 Fragilariaceae spp., Einarsson 1982). Thus, if there were an as yet unidentified driver of diatom
413 fluctuations, this driver would have to be strong enough to cause large fluctuations in benthic
414 primary production. Possible candidates for strong drivers are the mainly pelagic herbivore,
415 *Daphnia longispina*, and the epibenthic large-bodied cladocerans, and these do fluctuate in
416 synchrony with midges (Einarsson and Örnólfssdóttir 2004). Nonetheless, midges perform more
417 than 80% of the secondary production in the benthos (Lindegaard and Jónasson 1979), and
418 therefore are much better candidates for drivers of diatom abundance. Another possible candidate
419 for a driver of diatom fluctuations is *Anabaena* spp. that limit the growth of diatoms via shading.
420 Nonetheless, in the core data *Anabaena* spp. (as measured by echinenone) fluctuate in synchrony
421 with diatoms (diatoxanthin) (Table 1), which argues against shading from *Anabaena* spp. driving
422 diatom fluctuations.

423 The second general alternative hypothesis is that top-down forces generate fluctuations in
424 midges, and diatoms fluctuate in response. The obvious candidate for a top-down driver of midge
425 fluctuations is stickleback fish. Gut content analyses show that sticklebacks consume midges,
426 with midges comprising up to 56% of gut contents in a high-midge year and 9% in a low-midge
427 year (Gíslason et al. 1998). Nonetheless, the dominant midge, *T. gracilentus*, is better protected
428 than other midge species in their heavily constructed tubes and seems to be avoided by
429 sticklebacks. Furthermore, analyses of the time series of midges and sticklebacks (Einarsson et al.
430 2002) did not show the out-of-phase fluctuations that is expected for predator-prey cycles, instead
431 suggesting that sticklebacks follow rather than drive midge fluctuations. In addition to predators,
432 it is also possible that there is an unidentified parasite or pathogen that drives midge population
433 fluctuations, although we have little evidence for this.

434 Historical changes in grazing intensity and lake hydrology do not appear to have biased

435 the formation of the fossil record, nor the reliability of sedimentary time series as metrics of past
436 population abundance. Although intensification of herbivory is known to increase the rates of
437 deposition of algae and their pigments (Leavitt and Carpenter 1990), empirical (Leavitt et al.
438 1989) and modeling evidence (Cuddington and Leavitt 1999) show that this effect is limited to
439 less than a year in duration. Similarly, ecosystem-scale nutrient mass budgets reveal that over
440 90% of inflow silica is retained in the lake (Ólafsson 1979a), mainly due to uptake by and
441 deposition in diatoms (Opfergelt et al. 2011).

442

443 *Statistical Methods*

444 We developed a bootstrap method for determining the statistical significance of
445 correlations between two time series when each has temporal autocorrelation. Comparing its
446 results to standard correlations (Table 2) shows that standard correlations are likely to generate
447 type I errors (false positives). This can be explained simply with an example. Suppose there are
448 two 100-year time series that both show cycles with strict 10-year periods yet are independent.
449 There is a 20% chance that they fluctuate in either perfect synchrony or perfect asynchrony
450 (lagged by 5 years) for 100 years, which would clearly show very high statistical significance in a
451 standard correlation test; even if they were lagged by 1 or 6 years, the standard correlations
452 would likely be significant. Thus, it would be easy to get statistically significant correlations even
453 though we know that the time series are independent. Our bootstrap approach corrects for
454 autocorrelation and hence does not suffer from this potential source of type I errors.

455 Our state-space model takes a more-mechanistic approach, modeling explicit interactions
456 between variables and incorporating measurement error that accounts for sediment mixing. The
457 mathematical description of sediment mixing is simplistic, assuming that sediment layers below a
458 given strata have an influence that tapers off geometrically with depth. This is similar to the

459 assumption used by Blaauw and Christen (2011) to construct a model relating sediment depth to
460 age determined by radiocarbon dating. Nonetheless, there are numerous bioturbation (Kristensen
461 et al. 2012) models that incorporate much more sophisticated assumptions about the physical and
462 biological processes underlying sediment mixing (Sandnes et al. 2000, Meysman et al. 2005,
463 Schiffers et al. 2011). We have not attempted to incorporate the complexities of bioturbation into
464 our model, because the information needed to apply these approaches is unknown for our system.
465 Therefore, our approach matches the level of detail in the model to the data we have. When
466 applied to simulated data (Appendix A, online Supplemental Material), the approach did identify
467 the effects of sedimentation in smoothing the fluctuations in deposition rates. Despite this
468 smoothing effect, the state-space model still identified strong interactions between midges and
469 diatoms in both simulated and real data.

470

471 *Conclusion*

472 Our analyses of sediment core data give strong support to the midge-diatom consumer-
473 resource hypothesis to explain the fluctuations in midge and diatom abundances in Lake Mývatn.
474 Sediment cores are the only source of information about diatom fluctuations in Lake Mývatn,
475 because continuous long-term monitoring was not performed. Our example thus illustrates the
476 benefits of paleoecology to reconstruct history and extract missing information that is preserved
477 in sediment cores. This information is not limited to broad, ecosystem-level processes, but can
478 also be used to understand the population dynamical interactions between species.

479

480 ACKNOWLEDGMENTS

481 We thank Eva Pier for field assistance and Theodóra Matthíasdóttir for lab work. Two
482 anonymous reviewers provided great suggestions that improved this work. The study was funded

483 by the European Union “Eurolimpacs”-project GOCE-CT-2003-505540 and by Icelandic Centre
484 for Research (RANNÍS) grants no. 050219032 and 080010008. PL acknowledges funding from
485 NSERC (Natural Science and Engineering Research Council of Canada) and funding for ARI
486 was provided in part by US-NSF-DEB-LTREB-1052160.

487

488

REFERENCES

489 Aaby, B., and B. E. Berglund. 1986. Characterisation of peat and lake deposits. Pages 231-246 *in*

490 B. E. Berglund, editor. *Handbook of Holocene Palaeoecology and Palaeohydrology*. John
491 Wiley and Sons, Chichester, NY.

492 Berryman, A. A. 1976. Theoretical explanation of mountain pine beetle dynamics in lodgepole
493 pine forests. *Environmental Entomology* **5**:1225-1233.

494 Berryman, A. A., G. D. Amman, and R. W. Stark. 1978. Theory and practice of mountain pine
495 beetle management in lodgepole pine forests. Forest, Wildlife and Range Experimental
496 Station, University of Idaho, Moscow, Idaho, USA.

497 Blaauw, M., K. D. Bennett, and J. A. Christen. 2010. Random walk simulations of fossil proxy
498 data. *Holocene* **20**:645-649.

499 Blaauw, M., and J. A. Christen. 2011. Flexible paleoclimate age-depth models using an
500 autoregressive gamma process. *Bayesian Analysis* **6**:457-474.

501 Box, G. E. P., G. M. Jenkins, and G. C. Reinsel. 1994. *Time series analysis: forecasting and*
502 *control*. Third edition. Prentice Hall, Englewood Cliffs, New Jersey, USA.

503 Brinkhurst, R. O., K. E. Chua, and E. Batoosingh. 1969. Modifications in sampling procedures as
504 applied to studies on the bacteria and tubificid oligochaetes inhabiting aquatic sediments.
505 *Journal of the Fisheries Research Board of Canada* **26**: 2581-2593.

506 Carpenter, S. R., and P. R. Leavitt. 1991. Temporal variation in a paleolimnological record
507 arising from a trophic cascade. *Ecology* **72**: 277-285.

508 Cuddington, K., and P. R. Leavitt. 1999. An individual-based model of pigment flux in lakes:
509 Implications for organic biogeochemistry and paleoecology. *Canadian Journal of*
510 *Fisheries and Aquatic Science* **56**: 1964-1977.

511 Dennis, B., and B. Taper. 1994. Density dependence in time series observations of natural
512 populations: estimation and testing. *Ecological Monographs* **64**:205-224.

513 Dwyer, G., J. Dushoff, and S. H. Yee. 2004. The combined effects of pathogens and predators on
514 insect outbreaks. *Nature* **430**:341-345.

515 Efron, B., and R. J. Tibshirani. 1993. *An introduction to the bootstrap*. Chapman and Hall, New
516 York.

517 Einarsson, Á. 1982. The paleolimnology of Lake Myvatn, northern Iceland: plant and animal
518 micro-fossils in the sediment. *Freshwater Biology* **12**:63-82.

519 Einarsson, Á., A. Gardarsson, G. M. Gíslason, and A. R. Ives. 2002. Consumer-resource
520 interactions and cyclic population dynamics of *Tanytarsus gracilentus* (Diptera:
521 Chironomidae). *Journal of Animal Ecology* **71**:832-845.

522 Einarsson, Á., and R. D. Gulati, editors. 2004. *Ecology of Lake Myvatn and the River Laxa:*
523 *temporal and spatial variation*.

524 Einarsson, Á., and E. B. Örnólfsdóttir. 2004. Long-term changes in benthic Cladocera
525 populations in Lake Myvatn, Iceland. *Aquatic Ecology* **38**:253-262.

526 Einarsson, Á., G. Stefánsdóttir, H. Jóhannesson, J. S. Ólafsson, G. M. Gíslason, I. Wakana, G.
527 Gudbergsson, and A. Gardarsson. 2004. *The ecology of Lake Myvatn and the River Laxa:*
528 *Variation in space and time*. *Aquatic Ecology* **38**:317-348.

- 529 Gardarsson, A., Á. Einarsson, G. M. Gíslason, T. Hrafnisdóttir, H. R. Ingvason, E. Jónsson, and J.
530 S. Ólafsson. 2004. Population fluctuations of chironomid and simuliid Diptera at Myvatn
531 in 1977-1996. *Aquatic Ecology* **38**:209-217.
- 532 Gíslason, G. M., A. Gudmundsson, and Á. Einarsson. 1998. Population densities of the three-
533 spined stickleback (*Gasterosteus aculeatus* L.) in a shallow lake. *Verh Internat Verein*
534 *Limnol* **26**:2244-2250.
- 535 Håkanson, L., and M. Jansson. 1983. Principles of lake sedimentology. Springer, New York, NY.
- 536 Harvey, A. C. 1989. Forecasting, structural time series models and the Kalman filter. Cambridge
537 University Press, Cambridge, U.K.
- 538 Hauptfleisch, U., Á. Einarsson, T. J. Andersen, A. Newton, and A. Gardarsson. 2012. Matching
539 thirty years of ecosystem monitoring with a high resolution microfossil record.
540 *Freshwater Biology* **57**:1986-1997.
- 541 Holm, S. 1979. A simple sequentially rejective multiple test procedure. *Scandinavian Journal of*
542 *Statistics* **6**:65-70.
- 543 Ingvason, H. R., J. S. Ólafsson, and A. Gardarsson. 2004. Food selection of *Tanytarsus*
544 *gracilentus* larvae (Diptera: Chironomidae): an analysis of instars and cohorts. *Aquatic*
545 *Ecology* **38**:231-237.
- 546 Ives, A. R., K. C. Abbott, and N. L. Ziebarth. 2010. Analysis of ecological time series with
547 ARMA(p,q) models. *Ecology* **91**:858-871.
- 548 Ives, A. R., Á. Einarsson, V. A. A. Jansen, and A. Gardarsson. 2008. High-amplitude fluctuations
549 and alternative dynamical states of midges in Lake Myvatn. *Nature* **452**:84-87.
- 550 Jónasson, P. M., editor. 1979. Ecology of eutrophic, subarctic Lake Myvatn and the River Laxa.
551 *Oikos*.

552 Jónasson, P. M., and H. Adalsteinsson. 1979. Phytoplankton production in shallow eutrophic
553 Lake Myvatn, Iceland. *Oikos* **32**:113-138.

554 Kendall, B. E., C. J. Briggs, W. W. Murdoch, P. Turchin, S. P. Ellner, E. McCauley, R. M.
555 Nisbet, and S. N. Wood. 1999. Why do populations cycle? A synthesis of statistical and
556 mechanistic modeling approaches. *Ecology* **80**:1789-1805.

557 Krebs, C. J. 2011. Of lemmings and snowshoe hares: the ecology of northern Canada.
558 *Proceedings of the Royal Society B-Biological Sciences* **278**:481-489.

559 Krebs, C. J., S. Boutin, R. Boonstra, A. R. E. Sinclair, J. N. M. Smith, M. R. T. Dale, K. Martin,
560 and R. Turkington. 1995. Impact of food and predation on the snowshoe hare cycle.
561 *Science* **269**:1112-1115.

562 Kristensen, E., G. Penha-Lopes, M. Delefosse, T. Valdemarsen, C. O. Quintana, and G. T. Banta.
563 2012. What is bioturbation? The need for a precise definition for fauna in aquatic
564 sciences. *Marine Ecology Progress Series* **446**:285-302.

565 Leavitt, P. R., and S. R. Carpenter. 1989. Effects of sediment mixing and benthic algal
566 production on fossil pigment stratigraphies. *Journal of Paleolimnology* **2**:147-158.

567 Leavitt, P. R., S. R. Carpenter and J. F. Kitchell. 1989. Whole-lake experiments: The annual
568 record of fossil pigments and zooplankton. *Limnology and Oceanography* **34**: 700-717.

569 Leavitt, P. R., and D. A. Hodgson. 2001. Sedimentary pigments. Pages 295-325 in J. P. Smol, H.
570 J. B. Birks, and W. M. Last, editors. *Tracking environmental change using lake*
571 *sediments. V. 3: Terrestrial, algal and siliceous indicators.* Kluwer, Dordrecht, the
572 Netherlands

573 Lindegaard, C., and P. M. Jónasson. 1979. Abundance, population dynamics and production of
574 zoobenthos in Lake Mývatn, Iceland. *Oikos* **32**:202-227.

575 Lotka, A. J. 1925. *Elements of physical biology.* Williams and Wilkins, Baltimore, MD.

576 McCauley, E., W. A. Nelson, and R. M. Nisbet. 2008. Small-amplitude cycles emerge from
577 stage-structured interactions in Daphnia-algal systems. *Nature* **455**:1240-1243.

578 McCauley, E., R. M. Nisbet, W. W. Murdoch, A. M. de Roos, and W. S. C. Gurney. 1999. Large-
579 amplitude cycles of Daphnia and its algal prey in enriched environments. *Nature* **402**:653-
580 656.

581 Meysman, F. J. R., B. P. Boudreau, and J. J. Middelburg. 2005. Modeling reactive transport in
582 sediments subject to bioturbation and compaction. *Geochimica et Cosmochimica Acta*
583 **69**:3601-3617.

584 Murdoch, W. W., R. M. Nisbet, E. McCauley, A. M. deRoos, and W. S. C. Gurney. 1998.
585 Plankton abundance and dynamics across nutrient levels: Tests of hypotheses. *Ecology*
586 **79**:1339-1356.

587 Myers, J. H. 1988. Can a general hypothesis explain population cycles of forest Lepidoptera?
588 *Advances in Ecological Research* **18**:179-242.

589 Ólafsson, J. 1979a. The chemistry of Lake Mývatn and River Laxá. *Oikos* **32**:82-112.

590 Ólafsson, J. 1979b. Physical characteristics of Lake Mývatn and River Laxá. *Oikos* **32**:38-66.

591 Opfergelt, S., E. S. Eiríksdóttir, K. W. Burton, Á. Einarsson, C. Siebert, S. R. Gíslason, and A. N.
592 Halliday. 2011. Quantifying the impact of freshwater diatom productivity on silicon
593 isotopes and silicon fluxes: Lake Myvatn, Iceland. *Earth and Planetary Science Letters*
594 **305**:73-82.

595 Patoine, A., and P. R. Leavitt. 2006. Century-long synchrony of algal fossil pigments in a chain
596 of Canadian prairie lakes. *Ecology* **87**:1710-1721.

597 Sandnes, J., T. Forbes, R. Hansen, B. Sandnes, and B. Rygg. 2000. Bioturbation and irrigation in
598 natural sediments, described by animal-community parameters. *Marine Ecology Progress*
599 *Series* **197**:169-179.

- 600 Schiffers, K., L. R. Teal, J. M. J. Travis, and M. Solan. 2011. An Open Source Simulation Model
601 for Soil and Sediment Bioturbation. *PLoS ONE* **6**.
- 602 Schnurrenberger, D., J. Russell, and K. Kelts. 2003. Classification of lacustrine sediments based
603 on sedimentary components. *Journal of Paleolimnology* **29**:141-154.
- 604 Smol, J. P. 2010. The power of the past: using sediments to track the effects of multiple stressors
605 on lake ecosystems. *Freshwater Biology*, **55**: 43-59.
- 606 Stenseth, N. C. 1999. Population cycles in voles and lemmings: density dependence and phase
607 dependence in a stochastic world. *Oikos* **87**:427-461.
- 608 Thorarinsson, S. 1979. The postglacial history of the Mývatn area. *Oikos* **32**:17-28.
- 609 Thorbergsdóttir, I. M., S. R. Gíslason, H. R. Ingvason, and Á. Einarsson. 2004. Benthic oxygen
610 flux in the highly productive subarctic Lake Myvatn, Iceland: In situ benthic flux chamber
611 study. *Aquatic Ecology* **38**:177-189.
- 612 Troels-Smith, J. 1955. Karakterisering af løse jordarter. Danmarks Geologiske Undersøgelse,
613 Copenhagen.
- 614 Turchin, P. 2003. Complex population dynamics: a theoretical/empirical synthesis. Princeton
615 University Press, Princeton, NJ.
- 616 Turchin, P., and I. Hanski. 2001. Contrasting alternative hypotheses about rodent cycles by
617 translating them into parameterized models. *Ecology Letters* **4**:267-276.
- 618 Turchin, P., S. N. Wood, S. P. Ellner, B. E. Kendall, W. W. Murdoch, A. Fischlin, J. Casas, E.
619 McCauley, and C. J. Briggs. 2003. Dynamical effects of plant quality and parasitism on
620 population cycles of larch budmoth. *Ecology* **84**:1207-1214.

621
622 APPENDIX A

623 Simulation of midge and diatom abundance data.

624

625 APPENDIX B

626 Stratigraphy of pigments, loss on ignition (LOI), C, N, $\delta^{13}\text{C}$, diatoms, chironomid eggs and

627 Cladocera exuviae in the sediment cores.

628

629 Table 1: Correlations among six variables from two sediment cores.

	Midge				
	eggs	Dia	Echin	Allox	β -caro
Diatoxanthin	-0.37*				
Echinenone	-0.16	0.42*			
Alloxanthin	-0.03	0.25	0.34*		
β -carotene	-0.19	0.64**††	0.52**	-0.01	
Chlorophyll- <i>a</i>	0.09	0.53*	0.53*	0.17	0.77**††

630
 631 * $P < 0.05$, ** $P < 0.01$, calculated from a bootstrap that incorporates autocorrelation (Eq. 1)

632 † $P < 0.05$, †† $P < 0.01$, calculated from a bootstrap Holm-Bonferroni correct for multiple

633 comparisons that incorporates autocorrelation (Eq. 1)

634

635

636 Table 2: P-values (2-tailed and not corrected for multiple comparisons) from a standard Pearson
 637 correlation test (upper-right triangle) and from the bootstrap (Eq. 1) that accounts for temporal
 638 autocorrelation (lower-left triangle).

	Midge					
	eggs	Dia	Echin	Allox	β -caro	Chl- <i>a</i>
Midge eggs		0.012	0.29	0.87	0.20	0.52
Diatoxanthin	0.039		0.002	0.08	0.0000	0.0000
Echinenone	0.35	0.018		0.016	0.0001	0.0000
Alloxanthin	0.88	0.19	0.046		0.98	0.23
β -carotene	0.27	0.0001	0.003	0.96		0.0000
Chlorophyll- <i>a</i>	0.67	0.011	0.011	0.43	0.0003	

639

640 Table 3: Parameter estimates from the state-space model given by equations 2 and 3 for each of
 641 five pigments.

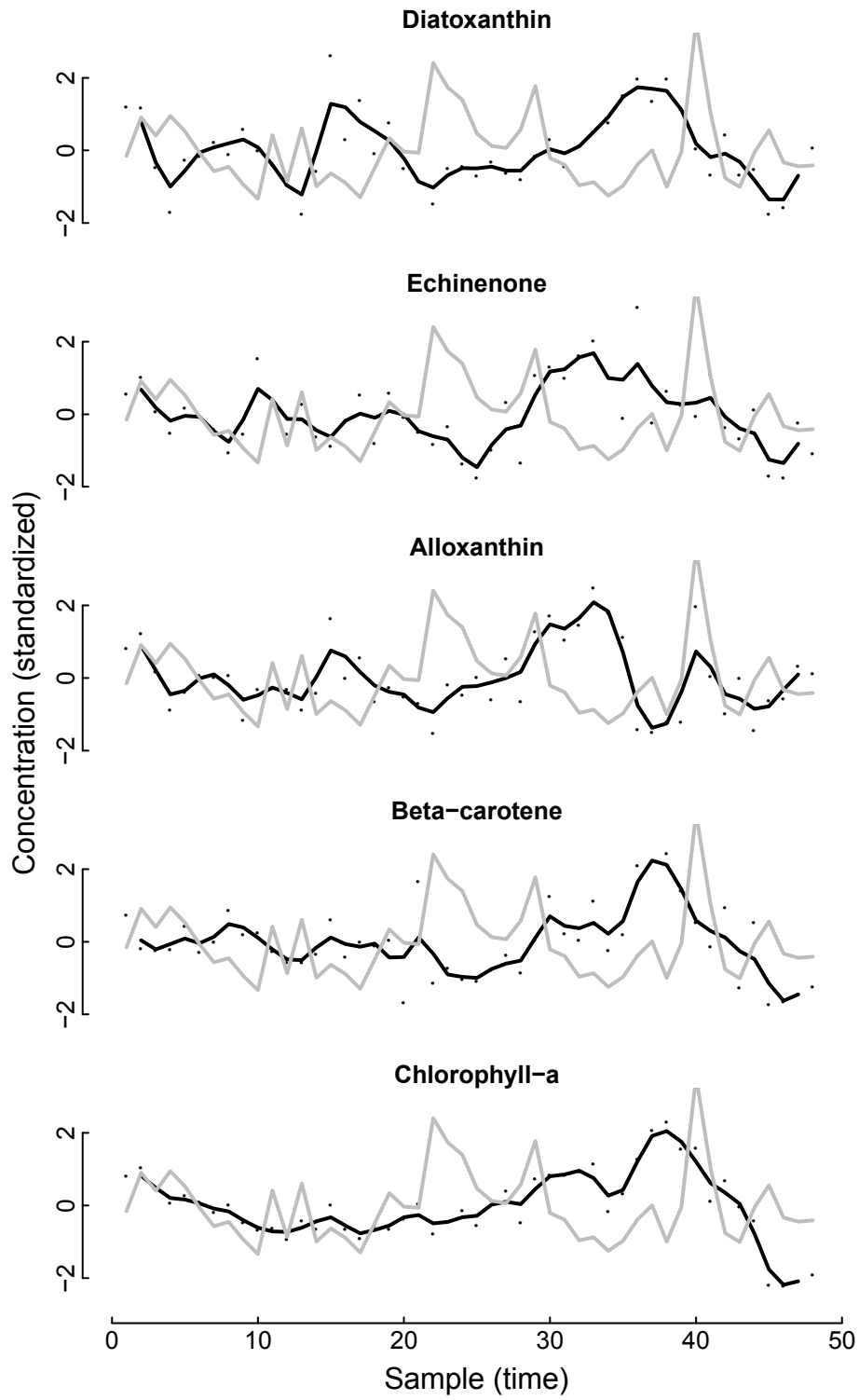
Coefficient	Diatoxanthin	Echinenone	Alloxanthin	$\tilde{\beta}$ carotene	Chl- <i>a</i>
b_{11}	-0.10	1.54	0.65	1.21	1.81
b_{22}	1.29	0.40	0.11	1.42	0.09
b_{12}	-0.90***	0.00	-0.10	-0.54**	-0.04
b_{21}	0.46*	-0.24	-0.31***	0.33*	0.65
b_{10}	0.36	0.75	0.21	0.32	0.89
b_{20}	-0.03	0.33	-0.08	-0.03	0.06
a	0.55	0.21	0.44	0.48	0.46
σ_1	0.39	0.00	0.38	0.00	0.00
σ_2	0.00	0.53	0.60	0.00	0.65
ν_1	0.00	-0.40	0.29	0.35	-0.17
ν_2	0.49	0.00	0.08	0.52	0.00
LL	-70.87	-79.76	-72.81	-73.68	-59.56
LRT χ^2_2	26.84	0.14	17.60	17.89	4.52
p-value	<0.0001	0.93	0.0002	<0.0001	0.10

642 *P < 0.05, **P < 0.01, ***P < 0.001

643

644
645 Fig. 1: Detrended sediment core data for midge egg capsules and diatoxanthin, echinenone,
646 alloxanthin, β -carotene, and chlorophyll-*a* (dots). Smoothing of midge (gray lines) and pigment
647 data (black lines) was performed to make fluctuating patterns in the data more clear; a direct form
648 II transposed filter was used with numerator coefficients (0.25, 0.5, 0.25), and denominator
649 coefficient 1.

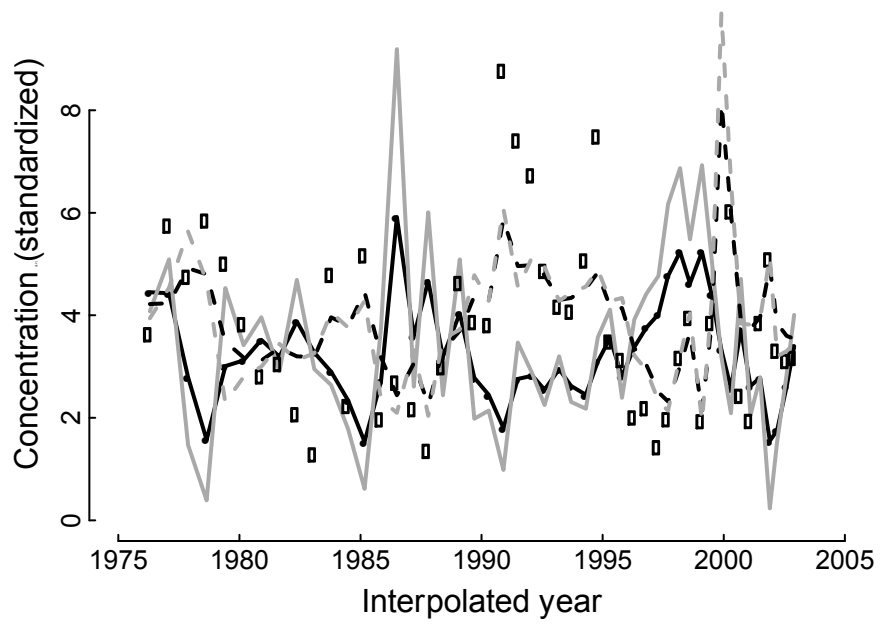
650
651 Fig. 2: Fit of the state-space model (Eqs. 2, 3) to detrended diatoxanthin (solid dots) and midge
652 egg capsule abundance (open dots). Solid and dashed black lines give the fit of the model to the
653 observed values $x^*(t)$ and $u^*(t)$ of diatoxanthin and midges (Eq. 3), whereas the solid and dashed
654 gray lines give the estimates of the deposition rates prior to sediment mixing (Eq. 2).



655

656

657



658

659

